



ORIGINAL ARTICLE

Exploratory study for the alkaline activation of basalt powder as a supplementary cementitious matrix

Estudo exploratório para ativação alcalina de pó basáltico como uma matriz cimentícia suplementar

Rafael Gheller^a Luciano Luiz Silva^a Márcio Antônio Fiori^a Eduardo Roberto Batiston^a ^aUniversidade Comunitária da Região de Chapecó – UNOCHAPECÓ, Department of Civil Engineering, Chapecó, SC, Brasil

Received 26 July 2021

Accepted 02 December 2021

Abstract: Portland cement remains the main material of choice in construction due to its thermal, mechanical and durability properties. However, there is growing concern about the large amount of energy consumed and the environmental pollution generated during its production. The objective of this study, therefore, was to evaluate the potential of the fine residual material produced by crushing basalt rocks to form a supplementary cementitious matrix through alkaline activation. Basalt powder with a particle size of less than 53 μ m was prepared and activated with a sodium hydroxide solution, with a sodium silicate solution as an adjuvant. The curing process of the material was also carried out at 5 temperature levels, 75, 85, 100, 115, 125°C, according to the experimental design. The paste was dry curing at a standard digital laboratory oven for 24 hours. After curing, the compressive strength of the material was evaluated, reaching a mean value of 10.21 MPa for the H5S15T125 mixture at 28 days. The microstructure analysis was performed by X-ray microtomography, presenting the reconstruction of the internal pores and cracks, leading to the conclusion that higher curing temperatures formed more porous matrices, although with more strength. Based on the collected data, the statistical analysis of the design was performed showing that sodium hydroxide and temperature have a statistically significant effect on the response variable compressive strength. As such, the alkali-activation of basalt powder can potentially produce a cementitious material of moderate strength, giving purpose to the residue and reducing the emission of harmful particles into the atmosphere.

Keywords: basalt, geopolymer, alkali-activated materials, cement.

Resumo: O cimento Portland continua sendo o principal material de escolha na construção civil, devido às suas propriedades térmicas, mecânicas e de durabilidade. No entanto, há uma crescente preocupação com a grande quantidade de energia consumida e a poluição ambiental gerada durante sua produção. Dessa forma, a presente pesquisa buscou avaliar o potencial do material residual fino produzido pela britagem de rochas basálticas através da ativação alcalina, para formar uma matriz cimentícia suplementar. O pó do basalto com tamanho de partículas menor que 53 μ m foi preparado e ativado com solução de hidróxido de sódio, tendo como coadjuvante a solução silicato de sódio. O material também teve o processo de cura realizado em 5 níveis de temperatura, 74,8, 85, 100, 115, 125,2°C conforme o delineamento experimental. Depois de curado o material teve a resistência à compressão avaliada, atingindo valor médio de 10,21 MPa para a mistura H5S15T125. A análise da microestrutura foi realizada através da microtomografia de raios X, apresentando a reconstrução dos poros e fissuras presentes internamente, concluindo que temperaturas de cura mais altas formaram matrizes mais porosas, embora com mais resistência. A partir dos dados coletados foi realizada a análise estatística do planejamento apresentando que hidróxido de sódio e a temperatura apresentam efeito estatisticamente significativo na variável resposta resistência à compressão. Portanto, é possível através da

Corresponding author: Rafael Gheller. E-mail: gheller@unochapeco.edu.br

Financial support: Institutional scholarship offered by the Universidade Comunitária da Região de Chapecó - Unochapecó.

Conflict of interest: Nothing to declare.

Data Availability: The data that support the findings of this study are available from the corresponding author, [RG], upon reasonable request. "SciELO Data" is available at <https://data.scielo.org/> if the authors wish to deposit Data at this multidisciplinary repository.



This is an Open Access article distributed under the terms of the Creative Commons Attribution License, which permits unrestricted use, distribution, and reproduction in any medium, provided the original work is properly cited.

álcali-ativação do pó de basalto produzir um material cimentício de resistência moderada, dando finalidade ao resíduo e diminuindo a emissão de partículas nocivas à atmosfera.

Palavras-chave: basalto, geopolímero, materiais álcali-ativados, cimento.

How to cite: R. Gheller, L. L. Silva, M. A. Fiori, and E. R. Batiston, "Exploratory study for the alkaline activation of basalt powder as a supplementary cementitious matrix," *Rev. IBRACON Estrut. Mater.*, vol. 15, no. 4, e15405, 2022, <https://doi.org/10.1590/S1983-41952022000400005>

1 INTRODUCTION

Civil construction uses several natural resources of the most varied types, and it generates great environmental impacts. However, it is a sector with room for technological innovation, be it in modern construction techniques or – especially – in high-performance materials. As such, new sources of raw material must be studied and used, as they could improve results in relation to performance and returns, consequently contributing to environmental issues.

From the perspective of reducing environmental impacts, it is known that Portland Cement is a major generator of harmful particles during its production. There is growing concern, therefore, about the large amount of energy consumed and the environmental pollution generated during its production. Research data from Rashad and Zeedan [1] reveal that for every ton of cement produced, approximately 0.8 tons of carbon dioxide are generated. The search for alternative cement materials that can reduce energy consumption and pollution has therefore become an important focus in several studies on this topic [2].

Unlike Portland cement, geopolymers are binders produced by the alkaline activation of aluminosilicate. These geopolymers tend to have similar performance as Portland cement and they are considered the most promising alternative for its replacement [3].

Alkaline activation is the synthesis reaction of the geopolymers. It is the hydration of aluminosilicates with alkaline or alkaline-earth substances, and there may be several aluminosilicate materials susceptible to this type of reaction [4]. Currently, most studies involving geopolymers look at materials such as blast furnace slag, fly ash and metakaolin [5]. However, new materials have been gaining attention in the research of new precursors, such as basalt [6]–[8].

In this sense, basalt is considered a potential raw material for the production of geopolymers, with essential elements for the alkali-activation process, the presence of silica and alumina in high levels, and, in some cases, with considerable amounts of vitreous material [6]–[10].

Basalts constitute the most common type of rock found on the Earth's surface. It is a volcanic igneous rock that covers about 70% of the planet's surface, and it's considered an industrial raw material with high potential due to its large-scale availability, high homogeneity, low impurities, high chemical stability, recyclability and non-toxic reactivity with water and air [11].

This material is widely consumed in civil construction, mainly as aggregate in concretes and for the foundation formation in pavements. Its processing, however, produces fine material residues that end up limiting some parameters of its use based on the Brazilian NBR 7211 standard [12], turning the powdery material into an unwanted waste for mining operations.

Studies by Drago et al. [13] have estimated that the amount of powdery material with a diameter of less than 0.075 mm in industrial sand is 7% to 20%, and this material is extracted in the washing method and generally goes unused in the crushing plant operation. These values represent a significant volume of fine material that could be susceptible to new applications.

In addition, the particle size reduced by grinding increases the reactivity of basalt due to the increase in its surface area. This makes basalt a promising material for the production of special cements by means of the alkali-activation process [6], [7], [11].

The improvement of a cementitious matrix is closely related to the microstructure of the material. Tortuous microstructures with narrow, isolated pores inhibit the diffusion of aggressive substances through the matrix, especially acids, carbonates or chlorides. Understanding the microstructural characteristics of the binder is therefore of vital importance to enable the incorporation of the alkali activation technology on a commercial scale [14]. The main microstructural properties of a binder include porosity, tortuosity, and the extent of pore network percolation [15], [16].

According to this problem definition, data from the National Association of Aggregate-Producing Entities for Construction (*Associação Nacional das Entidades de Produtores de Agregados para Construção*) [17] for the aggregates market reveal that in 2014 Brazil consumed the largest volume of aggregates ever, with an estimated consumption of 741 million tons of aggregates for concrete. And of this total, 302 million tons correspond to gravel,

extracted mainly from magmatic rocks. This means one must think about the amount of fine material waste generated, which often ends up being deposited in the yards of the crushing units.

Although non-toxic, the fine material ends up being carried by the water due to its fineness, carrying suspended debris, causing the silting of rivers and effluents, and it can also be carried by air. Resolution No. 307 [18] allowed instruments to move towards overcoming this reality, defining responsibilities and duties and making waste management mandatory in order to mitigate the environmental impacts arising from the uncontrolled activities related to the generation, transport and destination of these materials. It also determines that generators should adopt measures to reduce the generation of waste or to look for sources of reuse or recycling.

After the precursor element, alkaline activators are the essential component in the development of alkaline cement. In general terms, the activators used in aluminosilicate-based cement materials to generate high alkalinity are alkaline hydroxides, alkaline silicates or mixtures of both. The most commonly-used alkaline reagent solutions are based on a mixture of sodium hydroxides (NaOH) or potassium hydroxide (KOH) and silicate, sodium (Na₂SiO₃) or potassium (K₂SiO₃) solutions.

Geopolymerization then occurs in alkaline solutions with aluminosilicate oxides and silicates (solid or liquid) as reagents. Synthesis occurs through a mechanism that involves the dissolution of aluminum and silicon species from the surfaces of the base materials, as well as the surface hydration of the undissolved particles. Subsequently, the polymerization of active surface groups and soluble species occurs to form a gel, which then generates a hardened geopolymer structure. In most cases, only a small amount of the silica and alumina present in particles needs to dissolve and take part in the reaction for the entire mixture to solidify [19].

The objective of this work was to contribute to an alternative use of the fine material waste extracted from basalt, making it applicable as building material by forming a cement compound through its alkali-activation, transforming it into a product that can have some added value, reducing the environmental impact and developing innovative materials for civil construction. In addition, the interaction of three variables within the experiment was evaluated to achieve a reasonable compressive strength and seek an adequate characterization routine, after which the microstructural analysis using the X-ray microtomography technique was performed.

2 MATERIALS AND EXPERIMENTAL PROGRAM

The material used was established by basalt quarry waste, from the process of comminution of aggregates for civil construction in the western region of Santa Catarina, Brazil.

From Table 1, it is possible to observe some main chemical compounds for its mineral formation.

Table 1- Chemical composition of the basalt powder

Chemical composition, in oxides (%)	
SiO ₂	51,553
Fe ₂ O ₃	13,906
Al ₂ O ₃	13,091
CaO	8,846
MgO	4,159
TiO ₂	3,360
Na ₂ O	2,537
K ₂ O	1,583
P ₂ O ₅	0,435
MnO	0,190
Loss on ignition	<0,39

All the tests were carried out in controlled environments within the laboratories, evaluating the characteristics of the materials to optimize the strength of the materials, and analyzing their macro and micro structural characteristics to ensure the reliability of the experiment, following pre-established parameters to obtain the data.

Therefore, this is a 2³ factorial design, and response surface methodology (RSM) was used to obtain the optimal mixing proportions. Geometrically, the design is a cube, with 8 different treatments. This design allows 3 main effects (A,B,C) to be estimated together with the second-order interactions (AB, AC, BC) and one third-order interaction (ABC) [20]. Three factors were defined in the study: the cure temperature, the molarity of the NaOH solution, and the percentage of Na₂SiO₃ present in the alkaline solution.

The levels that each factor should be studied were specified to begin developing the research. Since it is a full 2³ composite factorial design, it will have eight tests that make up the factorial system, six axial points and one central point.

In the experimental design, the levels of each factor are represented by codes, which alternate until all possible combinations are formed.

To form the axial points of the design, the values of “α” are established as follows in Equation 1:

$$\alpha = (2^k)^{\frac{1}{4}} \Rightarrow \alpha = (2^3)^{\frac{1}{4}} \Rightarrow \alpha = 1,681 \tag{1}$$

Where α= the distance, in coded units, from each axial point in the factorial design, and k= number of factors involved in the experiment.

Values +1 and -1 represent the levels of each factor and make up the factorial system. The level encoded with the numeral 0 represents intermediate values of +1 and -1, and finally +α and -α will make up the axial points of the factors addressed in the study.

As can be seen in Table 1, a specific nomenclature is given to each mixture. This code has the function of helping in the identification of the material and can be explained as follows: for example, the mixture H5S15T125 is initially represented by the letter “H”, assigned to sodium hydroxide, followed by the numeral “5”, used to demonstrate the molarity of the solution. Next, “S15” represents the addition of 15% of the sodium silicate solution to the volume of the alkaline solution, and, finally, “T125” refers to the temperature, which was 125°C for this example.

A test design matrix had to be developed for the logical development of the study, so that mathematical models were applied with the collection of the results to evaluate the effects of the different mixtures established in the study. Table 2 presents the design matrix.

Table 2. Design Matrix 2^{k=3}

Tests	Sodium hydroxide (Mol/L)	Proportion of the NaSiO solution (%)	Temperature (°C)	Point	Nomenclature
1(1)	3 (-1)	9 (-1)	85 (-1)	Factorial	H3S9T85
2 (a)	7 (1)	9 (-1)	85 (-1)	Factorial	H7S9T85
3 (b)	3 (-1)	21 (1)	85 (-1)	Factorial	H3S21T85
4 (ab)	7 (1)	21 (1)	85 (-1)	Factorial	H7S21T85
5 (c)	3 (-1)	9 (-1)	115 (1)	Factorial	H3S9T115
6 (ac)	7 (1)	9 (-1)	115 (1)	Factorial	H7S9T115
7 (bc)	3 (-1)	21 (1)	115 (1)	Factorial	H3S21T115
8 (abc)	7 (1)	21 (1)	115 (1)	Factorial	H7S21T115
9	1,6 (+α)	15 (0)	100 (0)	Star	H1,6S15T100
10	8,3 (-α)	15 (0)	100 (0)	Star	H8, 3S15T100
11	5 (0)	25 (+α)	100 (0)	Star	H5S5T100
12	5 (0)	5 (-α)	100 (0)	Star	H5S25T100
13	5 (0)	15 (0)	75 (+α)	Star	H5S15T75
14	5 (0)	15 (0)	125(-α)	Star	H5S15T125
15	5 (0)	15 (0)	100 (0)	Central	H5S15T100

The experiment based on factorial schemes involves combinations between the levels of two or more factors. The proposed model considers the effect of a constant, the linear and quadratic effect of each of the independent variables, in addition to the effect of the interaction between them, which is presented later in the table of estimated effects.

The basalt powder with each alkaline solution proposed in the statistical model were mixed for 120 seconds, the period necessary for complete homogenization of the paste. Then, the filling of the molds took place in three layers, where for each layer, 20 compression movements with a socket were applied to improve the densification and then the excess material was flattened.

All mixtures underwent thermal curing for 24 hours, at a standard digital laboratory oven, hermetically insulated so that there is no rapid loss of water, posteriorly remained at room temperature until 28 days at room temperature, at which age they were ruptured, and their compressive strength was evaluated. For each mixture, at least 4 specimens were tested to collect compressive strength data.

2.1 X-ray Microtomography

X-ray microscopy (μ CT) is a recent technique that can be used in the three-dimensional reconstitution of solid materials to study crystallization processes, the origins of cracks and fissures, and the arrangement of pores and voids [21].

For this test, the samples of hardened basalt paste were prepared as disks with 5 mm thickness and 25 mm diameter and arranged in a container with silica gel and sealed to avoid moisture absorption. They were then sent to the Technological Characterization Laboratory (LCT) linked to the Department of Mining and Petroleum Engineering of the Polytechnic School of the University of São Paulo (USP).

The equipment used was the Zeiss Xradia Versa microtomograph, model XRM-510. This equipment uses the combination of a micrometric focus beam and image magnification in two stages: in the first step, the images are magnified through geometric magnification as in a conventional microtomograph; in the second step, a scintillator converts the X-rays to visible light and then magnifies the image optically through high contrast lenses, further enhancing the resolution of the sample's microstructure.

It is worth highlighting here that according to [22] it is possible to evaluate the pores through the three-dimensional reconstruction of the sample. These pores can be classified as open or closed, according to their disposition to an external fluid. Each type of pore is of influence on permeability, mechanical properties, density and conductivity. Pores can also be interconnected, further increasing the volume of voids and brittleness of the piece. In addition, surface roughness can also be considered as porosity.

In addition to the microtomography, analyzing the microstructure of the material is essential to reach conclusions about the material.

2.2. Mechanical Tests

The compressive strength test provides data on the strength of the material when subjected to controlled loads. In addition, it is possible to analyze the rupture interface and obtain data on the modulus of elasticity of the sample. The procedure of this test is adapted according to the Brazilian standard NBR 7215 [23], but since the cylindrical specimens have smaller dimensions (25 mm in diameter and 50 mm in length), the test speed and the applied force will be proportionally smaller.

The equipment used for this test was the Shimadzu Autograph AGX-Plus. For the test, a rotary joint was used to correct possible angular differences between the ends of the cylindrical specimen. A load at a constant speed of 0,03 kN/s was applied until the rupture of the geopolymer specimen. The age evaluated in the study was 28 days after molding.

Based on these data, the results were applied in the software STATISTICA, to validate the reliability of the study, presenting mathematical calculations to reveal which factors collaborated for a better performance of the material, and which levels and factors could be negligible in future research.

3 RESULTS AND DISCUSSION

3.1 Compressive Strength

The mean values for the compressive strength of each sample are presented in Table 3 for the tests in the first round and duplicate tests of the experimental design.

Table 3. Compressive strength results at 28 days

Tests	Nomenclature	Compressive strength in MPa (1st round)	Compressive strength in MPa (2nd round)
1(1)	H3S9T85	1,789	0,651
2 (a)	H7S9T85	1,759	1,959
3 (b)	H3S21T85	1,137	1,312
4 (ab)	H7S21T85	2,192	2,629
5 (c)	H3S9T115	3,190	5,567
6 (ac)	H7S9T115	7,473	6,997
7 (bc)	H3S21T115	4,441	8,292
8 (abc)	H7S21T115	7,946	5,639
9	H1,6S15T100	0,344	0,415
10	H8, 3S15T100	2,228	0,699
11	H5S5T100	4,432	2,447
12	H5S25T100	7,136	2,771
13	H5S15T75	5,431	3,504
14	H5S15T125	8,208	10,215
15	H5S15T100	4,781	2,395

The average values of compressive strength observed both in the first experiment and in the duplicate reveal that the molar variation presents maximum resistance values within the proposed range. Analytically, it is also possible to note that the increase in temperature in the two rounds of tests, contributing to the replicability and reliability of the experiment.

Using the response surface methodology to present the results, Figure 1 shows the tendency in the two-dimensional plane that - with increasing concentrations of sodium hydroxide or temperature - an increase in the compressive strength will occur, as represented by the color scale of the image.

The level curves represent the variation of compressive strength as a function of the independent variables that presented statistical significance in the study. As can be seen, the variables maintain their encoding of the design matrix and vary from $-\infty$ up to $+\infty$ for the evaluated points, indicated by blue circumferences.

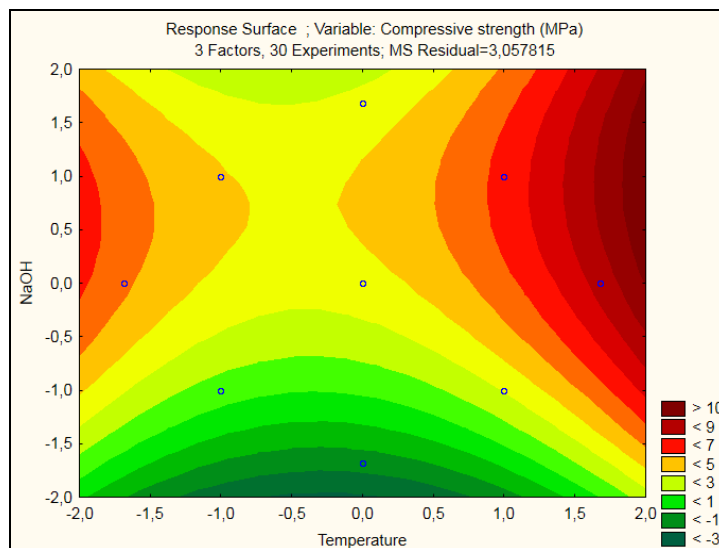


Figure 1. Temperature/NaOH response surface

Since there was no interaction between the independent variables, it is possible to make an analysis through the response surface methodology (RSM) according to each factor.

Figure 2 represents the surface three-dimensionally, where it is possible to see the curvature of the experiment effects using the quadratic equation that describes the experiment. The influence of NaOH concentration is worth highlighting at this point, which had a negative estimated effect for the quadratic effect. This phenomenon is visible on the response surface through the formation of a curvature that reaches a maximum point of the NaOH factor and soon after the strength values decrease as a function of the increase in the molarity of sodium hydroxide.

For the independent variable temperature, on the other hand, a positive or proportional correlation to compressive strength was revealed according to the proposed model and the calculation of estimated effects [6].

The variable sodium silicate did not correlate with compressive strength, so this phenomenon may be related to the chemical nature of basalt, and its subsequent use may be dispensed with.

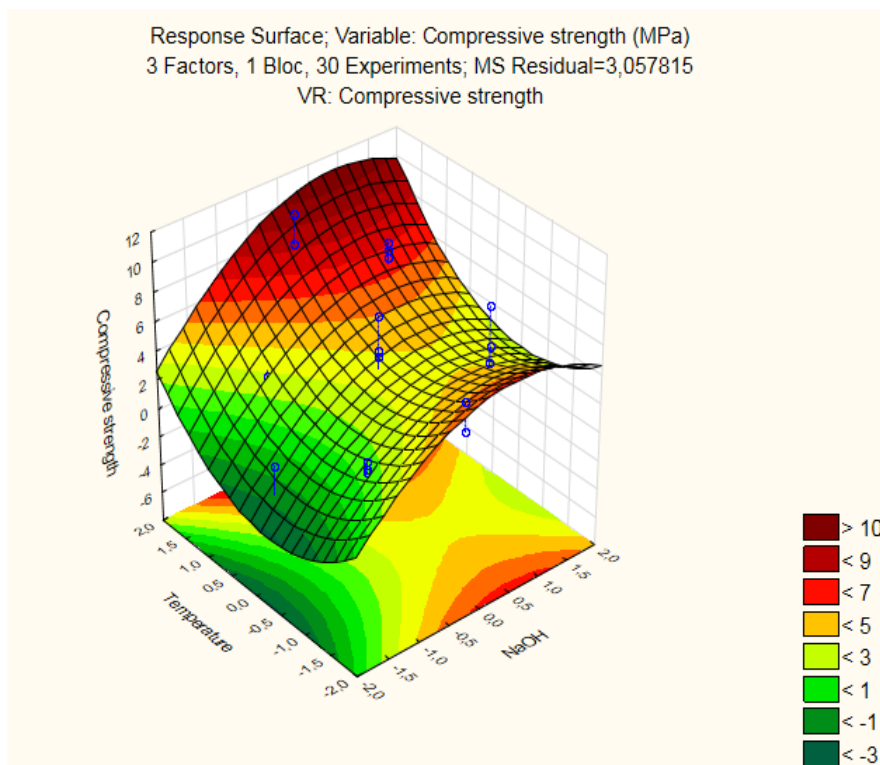


Figure 2. Response surface described by Equation 2 for the Temperature and NaOH variables.

3.2 X-ray Microtomography (μ CT)

For the microstructural imaging test performed through microtomography, samples of the mixtures were chosen that showed prominence in terms of compressive strength, since they encompass different levels of independent variables. The mixtures chosen were H7S9T85, H7S9T115, H5S15T125 and H5S15T100.

The advantage of this test is to evaluate the internal microstructure of the geopolymer and the arrangement of pores and cracks through a non-destructive method with minimal need for sample preparation.

The colors indicate the groups of interconnected pores and cracks, and distinct colors are not in communication with each other within the spatial distribution.

Figure 3 reconstructs the sample and distribution of voids in a 3D space of the quantified volume of sample H7S9T85 and the pixel size at acquisition corresponds to 19 μ m. The colors indicate the groups of interconnected pores and cracks, and distinct colors are not in communication with each other within the spatial distribution.

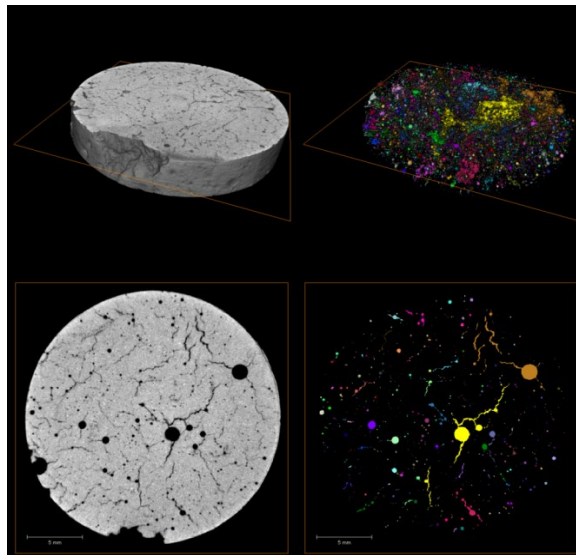


Figure 3. Generated images showing sample reconstitution and the distribution of voids in a 3D space of the quantified volume of sample H7S9T85.

The evaluation of sample H5S15T100 shows the image referring to the central point of the experiment. This experiment had an increase in the curing temperature, but a reduction in the concentration of the sodium hydroxide solution.

The 3D reconstruction reveals quite dispersed pores with voids and cracks that do not connect in large areas of the material, as can be ascertained through the color variation in the image.

The porosity of this sample was 3% of the volume and fewer cracks can be seen in the 2D plane, which may be related to a decrease in the amount of sodium hydroxide, an effect that is illustrated by Figure 4.

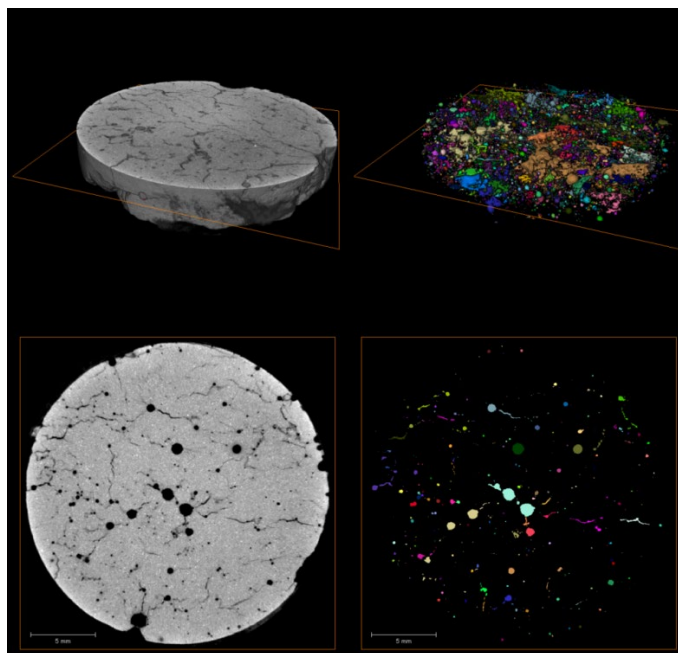


Figure 4. Generated images showing sample reconstitution and the distribution of voids in a 3D space of the quantified volume of sample H5S15T100.

Figure 5, on the other hand, visually demonstrates a significant increase in porosity, totaling a pore volume of 7%. Its compressive strength, however, was higher compared to the samples treated with lower temperatures.

Areas can be seen with larger volumes of interconnected pores represented by the same color, and on the 2D surface there is an increase in the presence of microcracks.

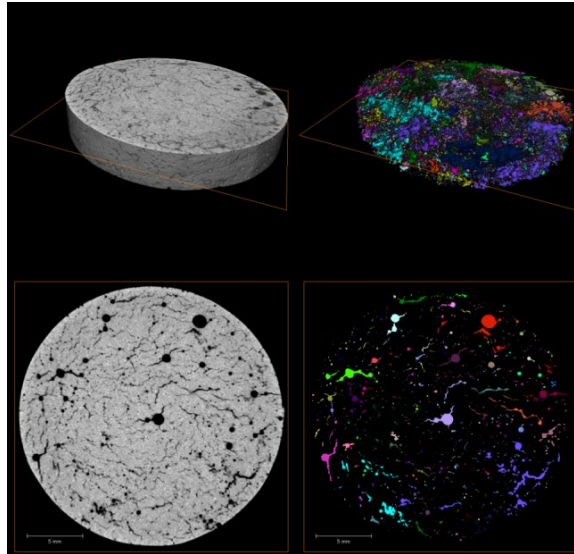


Figure 5. Generated images showing sample reconstitution and the distribution of voids in a 3D space of the quantified volume of sample H7S9T115.

And finally, sample H5S15T125, which is represented in Figure 6, had the highest amount of porosity, 9%. This representation reveals that the red color predominates in almost the entire porous fraction of the material, which shows that the voids are connected to each other within the geopolymeric matrix. In the 2D plane, the cracks show the retraction of the material due to heating and the loss of moisture with segmented voids throughout the sample.

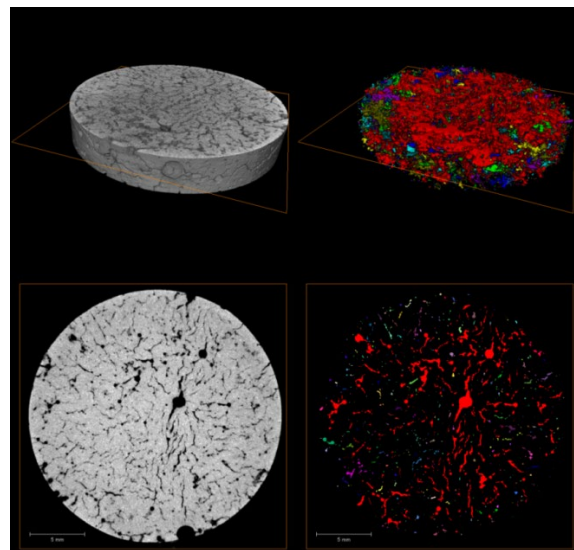


Figure 6. Generated images showing sample reconstitution and the distribution of voids in a 3D space of the quantified volume of sample H5S15T125.

But despite having a more porous material, this mixture was the one that showed the greatest compressive strength, reaching the mean value of 10.21 MPa. This phenomenon is linked to a synergy between temperature and molar concentration of the activator, presented on the response surface, mainly occurring in the first 24 hours.

The creation of bubbles can be associated with the reaction of reactive metal chemical elements (Al, Zn or Si) with the activation alkaline solution, releasing hydrogen gas bubbles and forming a complex network of pores [2]. Through the visual analysis, it is possible to identify a large variation in pore size, with micropores, mesopores and macropores at the interface, but it is necessary to focus on the reduction of macropores, since this has high relevance in relation to compressive strength.

The microstructural variability in the formation of the hardened material is affected by the variation of the factors under study, where the bond between the particles is affected by the physical and chemical properties of each mixture, or even by the electrostatic condition of the particle surface [24].

This study, therefore, provided the first systematic three-dimensional analysis of alkali-activated binder structures by X-ray microtomography and it provides an understanding of the distribution and geometry of the internal and external pore network in the sample, in a way that is not achievable using two-dimensional techniques such as scanning electron microscopy.

Thus, the obtained dataset provided information on porosity and pore geometry within the representative samples of the experiment. The three-dimensional reconstruction reveals primarily an interpretation of the pore chains, signaling that a greater thickening of the geopolymer in the curing process will bring more mechanical strength due to improvements in the transition zone and greater formation of binding gels. A denser matrix associated with temperature may have a beneficial synergic result for the geopolymer matrix.

On the other hand, when looking for a lighter and insulating material, it is important that the volume of voids remains or even increases. And in this regard, μ CT provides data on the homogeneity of the material so that future developments in this area are understood based on its microstructure.

As with most analytical techniques, μ CT has some significant limitations. Perhaps its biggest disadvantage is the compensation between resolution and sample size [15], [25].

Products with thermal curing at higher temperatures had an increase in porosity but their mechanical strength also increased significantly. Sample H5S15T125 is an example. It had a compressive strength of 8.20 MPa and 10.251 MPa in each round of the experiment, respectively, while its porosity was 9%. Table 4 shows the total volume of the samples and the volume of voids and their porosity as a percentage.

Table 4. Total pore volume measured by the complementary μ CT test and porosities as % of volume.

Sample	total vol (μm^3)	pore vol (μm^3)	porosity (%)
H7S9T85	1638300058968	60588942927	4%
H7S9T115	1737570000000	122993393055	7%
H5S15T125	1594880065183	137415146409	9%
H5S15T100	1584490150696	49512614886	3%

This behavior of the H5S15T125 sample is explained by the evaporation of water and the chemical changes of the hydration products resulting from the temperature rise, causing an increase in the porosity and pore size of the paste [26]. Although the increase in temperature potentiates the geopolymerization effect, the rapid exudation creates a thickening of the porous structure and the mechanical strength properties end up being affected [27].

It is estimated that the hardened binders contain pores with characteristic diameters that vary below the resolution used in the test, from 19 μm up to approximately 10 nm, which can lead to significant complexities in the geometry and distribution of the pores [28], [29]. However, in this research they presented crystallization even in samples with greater porosity, pointing out that a better thickening of the paste will improve mechanical strength.

4 CONCLUSIONS

Basalt rocks show potential for the development of alternative cements through the alkali-activation process. Although the compressive strength results were not high, it is possible to use this material in the addition of more reactive materials or even as a porous material for sound and thermal insulation purposes.

The statistical mathematical evaluation of the results revealed the existence of two independent variables (NaOH concentration and temperature) with a statistical significance in the strength gain of the material. Future research could expand the experimental design and obtain increases in mechanical strength.

In addition, due to the low emission of harmful gases and the composition of raw materials that cause less environmental impact compared to Portland cement, the product of this research has aspects of a promising material in civil construction.

The X-ray microtomography imaging revealed that the increase in curing temperature caused an increase in the porosity and number of cracks of the material, but higher temperatures formed a product of the basalt powder reaction with a material that was more resistant to axial compression.

Therefore, even with compressive strength values falling far short of the values obtained for other geopolymers based on metakaolin, blast furnace slag and some types of ash, the great advantage of the development of cementing materials with basalt rocks is the ease of obtaining the powdery material present in the aggregates, the abundance of raw material, and the aptitude for the alkali-activation process.

As this is an exploratory study, the study area was delimited to seek data on the mechanical strength and microstructure of the material. Future research should stipulate optimal proportions for alkaline reagents and additions so that maximum material performance is achieved, in addition to proposing an increase in the scale of production from laboratory to industrial scale.

Thus, the development of a matrix with additional cementitious materials from basalt powder is environmentally less aggressive due to low CO₂ emissions and economically viable, giving utility to a product of low added value, which is often discarded by mining companies in the region.

ACKNOWLEDGMENTS

The authors would like to thank the financial support offered by the Community University of the Region of Chapecó - Unochapecó.

REFERENCES

- [1] A. M. Rashad and S. R. Zeedan, "The effect of activator concentration on the residual strength of alkali-activated fly ash pastes subjected to thermal load," *Constr. Build. Mater.*, vol. 25, no. 7, pp. 3098–3107, 2011, <http://dx.doi.org/10.1016/j.conbuildmat.2010.12.044>.
- [2] H. Y. Zhang, V. Kodur, S. L. Qi, L. Cao, and B. Wu, "Development of metakaolin-fly ash based geopolymers for fire resistance applications," *Constr. Build. Mater.*, vol. 55, pp. 38–45, 2014, <http://dx.doi.org/10.1016/j.conbuildmat.2014.01.040>.
- [3] J. Davidovits, *Geopolymer Cement a Review* (Geopolymer Sci. Tech.). 2013.
- [4] C. G. S. Severo, D. L. Costa, I. M. T. Bezerra, R. R. Menezes, and G. A. Neves, "Características, particularidades e princípios científicos dos materiais ativados alcalinamente," *Rev. Eletrônica Mater. Process.*, vol. 8, no. 2, pp. 55–67, 2013.
- [5] P. Timakul, W. Rattanaprasit, and P. Aungkavattana, "Improving compressive strength of fly ash-based geopolymer composites by basalt fibers addition," *Ceram. Int.*, vol. 42, no. 5, pp. 6288–6295, 2016, <http://dx.doi.org/10.1016/j.ceramint.2016.01.014>.
- [6] M. Esaifan, M. Hourani, H. Khoury, H. Rahier, and J. Wastiels, "Synthesis of hydroxysodalite zeolite by alkali-activation of basalt powder rich in calc-plagioclase," *Adv. Powder Technol.*, vol. 28, no. 2, pp. 473–480, 2017, <http://dx.doi.org/10.1016/j.apt.2016.11.002>.
- [7] A. Solouki, G. Viscomi, R. Lamperti, and P. Tataranni, "Quarry waste as precursors in geopolymers for civil engineering applications: A decade in review," *Materials*, vol. 13, no. 14, pp. 3146, 2020, <http://dx.doi.org/10.3390/ma13143146>.
- [8] P. Tataranni, "Recycled waste powders for alkali-activated paving blocks for urban pavements: a full laboratory characterization," *Infrastructures*, vol. 4, no. 4, pp. 73, 2019., <http://dx.doi.org/10.3390/infrastructures4040073>.
- [9] A. Koppe, E. N. Guindani, and M. Mancini, "Avaliação do potencial de resíduo de rochas basálticas como matéria-prima para a produção de cimentos alternativos: processo de álcali-ativação," *Rev. Arquitetura IMED*, vol. 4, no. 2, pp. 24–32, 2015., <http://dx.doi.org/10.18256/2318-1109/arqimed.v4n2p24-32>.
- [10] P. Tataranni and C. Sangiorgi, "Synthetic aggregates for the production of innovative low impact porous layers for urban pavements," *Infrastructures Infrastructures*, vol. 4, no. 3, pp. 48, 2019., <http://dx.doi.org/10.3390/infrastructures4030048>.
- [11] H. Jamshaid and R. Mishra, "A green material from rock: basalt fiber: a review," *J. Textil. Inst.*, vol. 107, no. 7, pp. 923–937, 2016, <http://dx.doi.org/10.1080/00405000.2015.1071940>.
- [12] Associação Brasileira de Normas Técnicas, *Agregados para Concreto – Especificação*, ABNT NBR 7211:2009, 2009.
- [13] C. Drago, J. C. K. Verney, and F. M. Pereira, "Efeito da utilização de areia de britagem em concretos de cimento Portland," *Rem Rev. Esc. Minas*, vol. 62, no. 3, pp. 399–408, 2009, <http://dx.doi.org/10.1590/S0370-44672009000300021>.

- [14] J. S. J. Van Deventer, J. L. Provis, P. Duxson, and D. G. Brice, "Chemical research and climate change as drivers in the commercial adoption of alkali activated materials," *Waste Biomass Valoriz.*, vol. 1, no. 1, pp. 145–155, 2010, <http://dx.doi.org/10.1007/s12649-010-9015-9>.
- [15] J. L. Provis, R. J. Myers, C. E. White, V. Rose, and J. S. J. Van Deventer, "X-ray microtomography shows pore structure and tortuosity in alkali-activated binders," *Cement Concr. Res.*, vol. 42, no. 6, pp. 855–864, 2012, <http://dx.doi.org/10.1016/j.cemconres.2012.03.004>.
- [16] M. A. B. Promentilla, T. Sugiyama, T. Hitomi, and N. Takeda, "Quantification of tortuosity in hardened cement pastes using synchrotron-based X-ray computed microtomography," *Cement Concr. Res.*, vol. 39, no. 6, pp. 548–557, 2009, <http://dx.doi.org/10.1016/j.cemconres.2009.03.005>.
- [17] Associação Nacional das Entidades de Produtores de Agregados para Construção, "Areia de brita para construção: Evolução de processos e mudanças estruturais nos grandes centros urbanos favorecem utilização do produto para o mercado," *Rev. Areia Brita*, pp. 20–24, 2018.
- [18] Brasil, *Resolução nº 307, de 5 de Julho de 2002*, 2002.
- [19] E. Álvarez-Ayuso et al., "Environmental, physical and structural characterisation of geopolymer matrixes synthesised from coal (co-)combustion fly ashes," *J. Hazard. Mater.*, vol. 154, no. 1-3, pp. 175–183, 2008, <http://dx.doi.org/10.1016/j.jhazmat.2007.10.008>.
- [20] D. C. Montgomery, G. C. Runger, and N. F. Hubele, *Estatística Aplicada à Engenharia*, 2a ed. Rio de Janeiro: LTC, 2004.
- [21] L. C. Briese, S. Selle, C. Patzig, J. Deubener, and T. Höche, "Depth-profiling of nickel nanocrystal populations in a borosilicate glass: a combined TEM and XRM study," *Ultramicroscopy*, vol. 205, pp. 39–48, 2019, <http://dx.doi.org/10.1016/j.ultramic.2019.06.004>.
- [22] O. L. Alves, I. F. Gimenez, and O. P. Ferreira, "Desenvolvimento de ecomateriais: materiais porosos para aplicação em Green Chemistry (Química Verde)," in *Química Verde en Latinoamérica*, P. Tundo and R. H. Rossi, Eds., Buenos Aires: IUPAC, 2004.
- [23] Associação Brasileira de Normas Técnicas, *Cimento Portland – Determinação da Resistência à Compressão de Corpos de Prova Cilíndricos*, ABNT NBR 7215, 2019.
- [24] M. Dobiszewska, A. K. Schindler, and W. Pichór, "Mechanical properties and interfacial transition zone microstructure of concrete with waste basalt powder addition," *Constr. Build. Mater.*, vol. 177, pp. 222–229, 2018, <http://dx.doi.org/10.1016/j.conbuildmat.2018.05.133>.
- [25] U. Rattanasak and K. Kendall, "Pore structure of cement/pozzolan composites by X-ray microtomography," *Cement Concr. Res.*, vol. 35, no. 4, pp. 637–640, 2005, <http://dx.doi.org/10.1016/j.cemconres.2004.04.022>.
- [26] C. Medina, M. Frías, M. I. Sánchez De Rojas, C. Thomas, and J. A. Polanco, "Gas permeability in concrete containing recycled ceramic sanitary ware aggregate," *Constr. Build. Mater.*, vol. 37, pp. 597–605, 2012, <http://dx.doi.org/10.1016/j.conbuildmat.2012.08.023>.
- [27] W. Franus, A. Halicka, K. Lamorski, and G. Jozefaciuk, "Microstructural differences in response of thermoresistant (ceramic) and standard (granite) concretes on heating. studies using SEM and nonstandard approaches to microtomography and mercury intrusion porosimetry data," *Materials*, vol. 11, no. 7, pp. 1126, 2018, <http://dx.doi.org/10.3390/ma11071126>.
- [28] F. Collins and J. G. Sanjayan, "Effect of pore size distribution on drying shrinkage of alkali-activated slag concrete," *Cement Concr. Res.*, vol. 30, no. 9, pp. 1401–1406, 2000, [http://dx.doi.org/10.1016/S0008-8846\(00\)00327-6](http://dx.doi.org/10.1016/S0008-8846(00)00327-6).
- [29] W. M. Kriven, J. L. Bell, and M. Gordon, "Microstructure and nanoporosity of as-set geopolymers," in *Mechanical Properties and Performance of Engineering Ceramics II*, R. Tandon, A. Wereszczak, and E. Lara-Curzio, Eds., Hoboken: Wiley, 2008.

Author contributions: RG and ERB: conceptualization, methodology, supervision, writing; LLS and MAF: conceptualization, data curation, formal analysis and review of article writing.

Editors: Edna Possan, Guilherme Aris Parsekian.